Article

Oxidation-Triggered Release of Fluorescent Molecules or Drugs from Mesoporous Si Microparticles

Elizabeth C. Wu, Ji-Ho Park, Jennifer Park, Ester Segal, Fre#de#rique Cunin, and Michael J. Sailor

ACS Nano, **2008**, 2 (11), 2401-2409 • Publication Date (Web): 08 November 2008

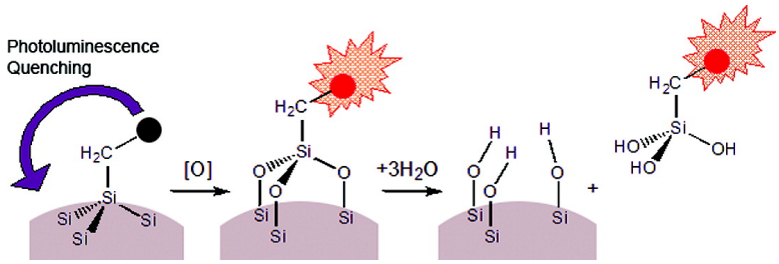

More About This Article

Additional resources and features associated with this article are available within the HTML version:

- Supporting Information
- Access to high resolution figures
- Links to articles and content related to this article
- Copyright permission to reproduce figures and/or text from this article

View the Full Text HTML

Oxidation-Triggered Release of Fluorescent Molecules or Drugs from Mesoporous Si Microparticles

Elizabeth C. Wu,[†] Ji-Ho Park,[‡] Jennifer Park,[†] Ester Segal,[§] Frédérique Cunin,[⊥] and Michael J. Sailor[†,‡,§,*]

[†]Department of Bioengineering, [‡]Materials Science and Engineering Program, and [§]Department of Chemistry and Biochemistry, University of California, San Diego, 9500 Gilman Drive, La Jolla, California 92093, and [⊥]Institute Charles Gerhardt Montpellier, UMR 5253 CNRS-UM2-ENSCM-UMI, Materiaux Avances pour la Catalyse et la Sante Montpellier, France

ABSTRACT The fluorescent dye Alexa Fluor 488 or the anticancer drug doxorubicin is attached to the surface and inner pore walls of mesoporous Si particles by covalent attachment, and the oxidation-induced release of each molecule is studied. The molecules are bound to the Si matrix using a 10-undecenoic acid linker, which is attached by thermal hydrosilylation. Loading capacity of the microparticles using this method is ~0.5 and 45 mg/g of porous Si microparticle for Alexa Fluor 488 and doxorubicin, respectively. The Si—C-bound assembly is initially stable in aqueous solution, although oxidation of the underlying Si matrix results in conversion to silicon oxide and slow release of the linker—molecule complex by hydrolysis of the Si—O attachment points. When the attached molecule is a fluorophore (Alexa Fluor 488 or doxorubicin), its fluorescence is effectively quenched by the semiconducting silicon matrix. As the particle oxidizes in water, the fluorescence intensity of the attached dye increases due to growth of the insulating silicon oxide layer and, ultimately, dye release from the surface. The recovery of fluorescence in the microparticle and the release of the molecule into solution are monitored in real-time by fluorescence microscopy. Both processes are accelerated by introduction of the oxidizing species peroxynitrite to the aqueous solution. The oxidation-triggered release of the anticancer drug doxorubicin to HeLa cells is demonstrated.

KEYWORDS: microparticles · drug loading · controlled drug release · cancer therapy · fluorescence resonant energy transfer · nanotechnology

Traditional methods of drug administration, such as oral delivery or injection, usually result in rapid release and clearance of the drug.[1] A high initial drug dose is therefore necessary in order to maintain a therapeutic concentration over a period of time, which may produce toxic side effects.[1,2] Controlled drug release technologies can improve the efficacy of traditional drug therapies by reducing the systemic concentration of free drug.[3] Various drug delivery vehicles have been employed, such as liposomes,[4] micelles,[5] gelatin nanoparticles,[6] solid lipid nanoparticles,[7] silica-based nanoparticles,[8] and porous Si.[9−15] Porous Si possesses several properties that make it advantageous as a drug delivery system, including low toxicity,[11,16−19] a high surface area,[20] and tunable pore sizes and volumes.[20] Chemical modification of the porous Si surface can also be achieved,[21] providing many means to adjust the chemical stability of the material as well as to load a particular drug of interest. As with all biodegradable drug delivery carriers, the toxicity of the degradation products is an important factor. Si is an essential trace element that is required for proper bone and collagen growth.[22] The bioavailable form of silicon consists of various oxo anions of orthosilicic acid ($Si(OH)_4$), which are rapidly removed by the kidneys in the human body.[23] This is also the primary degradation product of porous Si in aqueous media, and the rate of production of orthosilicic acid is dependent on the porosity of the porous Si sample.[22]

A variety of drugs such as ibuprofen,[24] dexamethasone,[25] and doxorubicin[15] have been placed in porous Si matrices. In most reports, drug loading is accomplished by adsorption of the drug to the inner pore walls of a suitably modified porous Si sample. These preparations typically release the drug rapidly. For long-term drug delivery applications, it is desirable to minimize rates of desorption and leaching of drug from the fixture; one means to accomplish this is to attach the drug to the porous Si matrix by covalent attachment. This approach offers the added possibility of triggering release by incorporating a physiologically responsive linker, for example, an enzyme-cleavable peptide sequence.[26] The method described here uses covalent attachment to load Alexa Fluor 488 or doxorubicin into porous Si microparticles. Alexa Fluor 488 is a stable fluorescent molecule that is used in this study to model drug release. Doxorubicin is an anticancer agent that also possesses intrinsic fluorescence properties. The model drugs are attached to a linker and grafted to the porous Si

*Address correspondence to msailor@ucsd.edu.

Received for review September 17, 2008 and accepted October 25, 2008.

Published online November 8, 2008. 10.1021/nn800592q CCC: $40.75

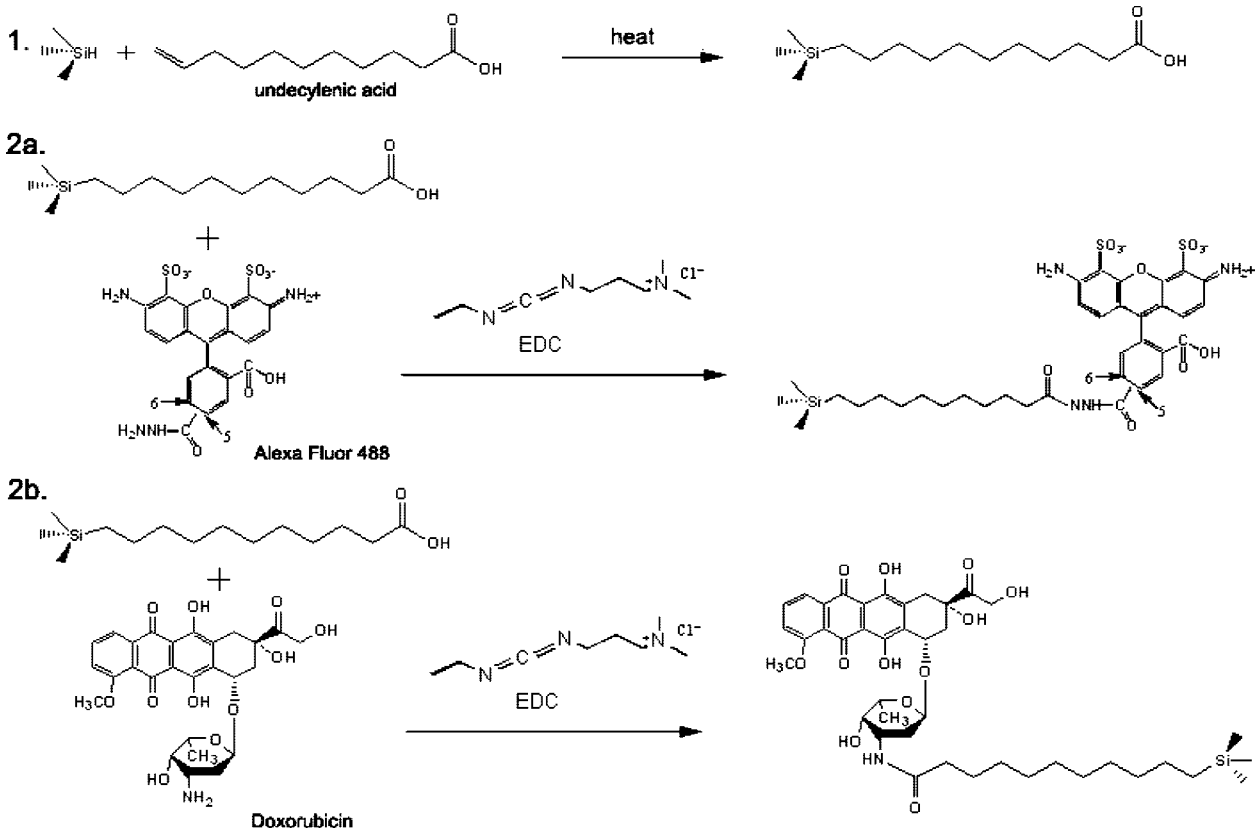

Scheme 1. Loading of molecular payloads in porous Si microparticles by covalent attachment. The process involves functionalization of the porous Si surface by thermal hydrosilylation of undecylenic acid (1), followed by EDC-mediated coupling of either the fluorescent molecule Alexa Fluor 488 (2a) or the anticancer drug doxorubicin (2b).

surface by means of Si−C bonds. The Si−C surface bond is stable in aqueous media; however, the Si−Si back bonds of the assembly can be oxidized,[21] resulting in insertion of oxygen to form Si−O−Si linkages. Unlike the Si−C bond, the Si−O bond is susceptible to hydrolysis in aqueous media.[21] Thus, oxidation of the underlying Si matrix can result in oxidation-triggered release of the linker−molecule complex.

A second unique aspect of the porous Si system is the ability of the material to efficiently quench photoluminescence from a fluorophore by energy transfer. We find that oxidation of porous Si eliminates the quenching pathway, providing a means to monitor the progress of oxidatively triggered drug or molecule delivery. We show that the process is accelerated in the presence of biologically relevant reactive oxygen species (ROS).

In this study, doxorubicin was used as a test drug. Doxorubicin is a highly toxic drug that is used for chemotherapy and has a narrow therapeutic concentration range due to undesirable side effects such as cardiotoxicity and myelosuppression.[27] The covalent method described here allows for drug release only when the covalent bonds are broken or when the porous Si matrix is oxidized and degraded. We observe a significant, extended release of doxorubicin that is covalently attached to the porous Si matrix compared to doxorubicin that is physically adsorbed onto the porous Si matrix. We conclude that loading porous Si microparticles with a drug through covalent attachment is a viable candidate for long-term drug release applications.

RESULTS AND DISCUSSION

Porous Si films were synthesized by electrochemical etching of highly doped p-type Si wafers in an aqueous electrolyte containing HF and ethanol. The resulting porous film was lifted off and fractured into microparticles using ultrasound.[28] Freshly etched porous Si is unstable in aqueous media due to oxidation of the reactive surface hydrides, and therefore, surface modification is necessary in order to improve stability.[29,30] Step 1 in Scheme 1 illustrates functionalization of the freshly etched microparticles using microwave-assisted thermal hydrosilylation with undecylenic acid, in which a Si−C linkage is created.[31] The molecules Alexa Fluor 488 or doxorubicin were then grafted to the carboxy terminus of the modified surface. 1-Ethyl-3-[3-dimethylaminopropyl]carbodiimide hydrochloride (EDC) was used to link the hydrazide group of Alexa Fluor 488 to the carboxylic acid group on the porous Si surface. Doxorubicin was attached to the porous Si microparticles in a similar manner, *via* the primary amine of doxorubicin. In both attachment chemistries, an amide bond is formed (Scheme 1).

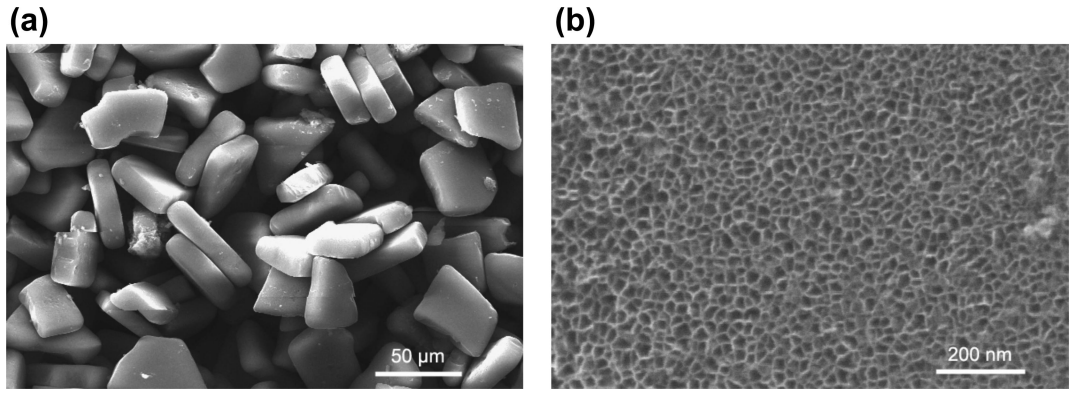

Figure 1. (a) Scanning electron microscope (SEM) image of a representative sample of porous Si microparticles. (b) A close-up SEM view of one of the microparticles, revealing the mesoporous structure.

Scanning electron microscope images reveal that, after ultrasonic fracture and chemical modification, the porous Si sample consists of microparticles with sizes in the range of 30−50 μm (Figure 1a). Each individual microparticle is permeated with mesopores of 20−30 nm diameter (Figure 1b). The specific surface area, the porous volume, and the pore size of the microparticles were determined using nitrogen adsorption measurements with the application of the BET (Brunauer−Emmett−Teller) and the BdB (Broekhof−de Boer) methods.[32−34] The hysteresis loop observed is associated with cylindrically shaped pores of approximately constant cross section. The average pore diameter was calculated to be 20 ± 3 nm for the chemically modified microparticles, consistent with the SEM images. The surface area (S_{BET}) was ~260 m^2 (STP)/g, and the porous volume was ~780 cm^3 (STP)/g.

Covalent attachment of the dye and drug was confirmed by Fourier transform infrared (FTIR) spectroscopy. The FTIR spectrum of freshly etched porous Si microparticles displays bands characteristic of surface hydride species (Figure 2a). A band at 2110 cm^{-1} associated with the ν_{Si-H} stretching vibrations, a band corresponding to the δ_{Si-H2} scissors mode at 910 cm^{-1}, and a band corresponding to a ν_{Si-H} deformation mode (663 cm^{-1}) are apparent in the spectrum. After hydrosilylation with undecylenic acid, bands at 2928 and 2857 cm^{-1} associated with ν_{C-H} stretching modes and a band at 1715 cm^{-1} associated with the $\nu_{C=O}$ stretching mode are observed (Figure 2b). Conjugation of the drug or dye molecules generates bands in the FTIR spectrum characteristic of amide I (1655 cm^{-1}) and amide II (1588 cm^{-1}), indicative of the formation of the linking amide bond (Figure 2c).[35]

The photophysical interaction of the fluorophore Alexa Fluor 488 with the porous Si matrix was measured by fluorescence microscopy. The degree of fluorescence quenching relates to the extent of oxidation of the porous Si microparticles. In the as-prepared material, very low levels of fluorescence are observed from the dye grafted onto porous Si (Figure 3a). The weak fluorescence intensity is attributed to the high density of electronic states in the semiconductor, which efficiently quenches the excited state of the attached fluorophore. The system can be thought of as a solid-state analogue of fluorescence resonance energy transfer (FRET), where the attached dye is the energy donor and the porous Si matrix is the acceptor. The exchange of energy between quantum dot−molecular dye conjugates has been observed previously,[36] and it appears to be a general feature of systems where the donor−acceptor separation distance is small.[37] In the specific case of porous Si, the quenching of fluorescence from dye molecules has been well-studied by Vial[38−40] and others.[41,42]

As the porous Si microparticles oxidize in aqueous solution (pH 10), the growing oxide layer increases the separation between the dye donor and the semiconductor acceptor, resulting in a steady increase in photoluminescence intensity associated with the particles. A 10-fold increase in the intensity of dye fluorescence is

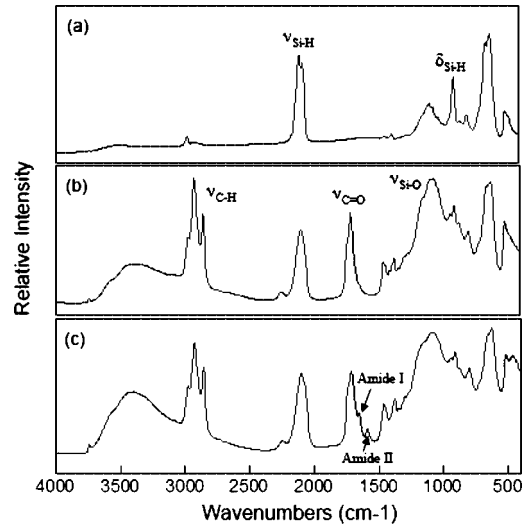

Figure 2. Diffuse-reflectance Fourier transform infrared spectra of porous microparticles corresponding to the chemical transformation steps of Scheme 1. (a) Freshly etched porous Si before chemical modification. (b) Porous Si microparticles after hydrosilylation with undecylenic acid. (c) Particles after attachment of Alexa Fluor 488. The *y*-axis is presented in relative Kubelka−Munk units.

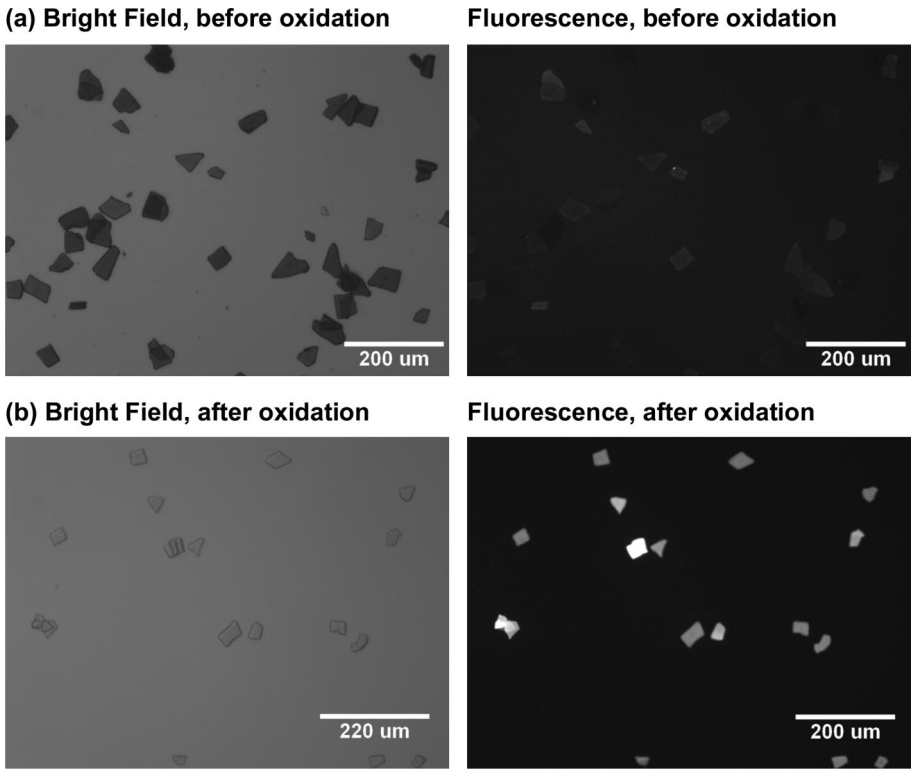

Figure 3. Microscope images of porous Si microparticles with Alexa Fluor 488 attached, showing the increase in fluorescence intensity as the porous Si microparticles oxidize. (a) Bright-field (left) and fluorescence (right) images of the microparticles before oxidation. (b) Bright-field (left) and fluorescence (right) images after treatment with pH 10 buffer for 5 days, showing the significant increase in fluorescence intensity from the attached dye when the porous Si matrix oxidizes. Fluorescence images were obtained using 480 nm excitation and 535 ± 25 nm observation channels.

measured (MetaMorph image analysis software, average of 10−20 particles) after 24 h and a 30-fold increase is observed after a few days (Figure 3). Oxidation of the porous Si matrix was verified *ex situ* by the appearance of a broad band centered at 1000 cm^{-1} in the FTIR spectrum, associated with silicon oxide stretching modes. Independent measurements verified that the intensity of fluorescence of the Alexa Fluor 488 dye itself is independent of pH in the range of 7−10. The increase in fluorescence intensity measured from the dye-modified porous Si microparticles provides a convenient means to monitor the extent of oxidation of the porous Si constituent, the first step in the aqueous dissolution of the fixture.

Covalent attachment allows the grafted molecule to be released only after the silicon host matrix dissolves. Degradation of porous silicon in aqueous solutions in the physiological pH range involves the oxidation of silicon into silicon dioxide (eq 1), followed by hydrolysis with water (eq 2) to release orthosilicic acid.[22]

$$Si + O_2 \rightarrow SiO_2 \quad (1)$$

$$SiO_2 + 2H_2O \rightarrow Si(OH)_4 \quad (2)$$

The first step in this process, the oxidation of Si, occurs in aqueous solutions such as phosphate-buffered saline (PBS) or in cell media, although the reaction is slow. Oxidation can be accelerated by the addition of an oxidizing agent such as reactive oxygen species (ROS), in particular peroxynitrite ($ONOO^-$).

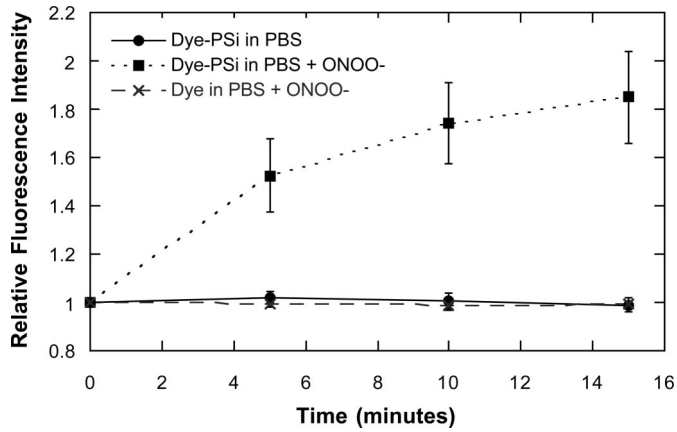

Figure 4. Comparison of the change in fluorescence intensity of an Alexa Fluor 488 dye grafted to porous Si microparticles as a function of time after addition of peroxynitrite ($ONOO^-$). Controls with pure buffer (PBS) and with free dye (not attached to porous Si) are shown for comparison. The data are quantified by fluorescence microscopic measurement of the microparticles and presented as the ratio of fluorescence intensity relative to the fluorescence intensity measured at time $t = 0$. The 535 ± 25 nm emission channel is monitored using 480 nm excitation.

Peroxynitrite, a biologically significant ROS, is a strong oxidant that is synthesized *in vivo* when superoxide and nitric oxide (NO) are generated in close proximity.[43] Peroxynitrite is thought to produce oxidative damage in tissues by oxidizing or nitrating biological molecules such as tyrosine.[44] In this study, 1−2 mM of 3-morpholinosydnomine (SIN-1) was used to generate physiologically relevant micromolar levels of $ONOO^-$ *in situ*, in a pH 7 buffer solution (PBS).[45,46] As observed with the base-induced oxidation, oxidation by $ONOO^-$ increases the fluorescence intensity of the microparticles (Figure 4), but only by a factor of ~2. However, the reaction is faster than base-induced oxidation, and fluorescence intensity increases significantly within the first 15 min of exposure. Control experiments with PBS buffer show a much smaller rate of fluorescence increase. A control experiment involving incubation of free Alexa Fluor 488 with $ONOO^-$ does not produce a measurable change in fluorescence intensity on this time scale. As with base-induced oxidation, the recovery of fluorescence intensity is attributed to a reduction

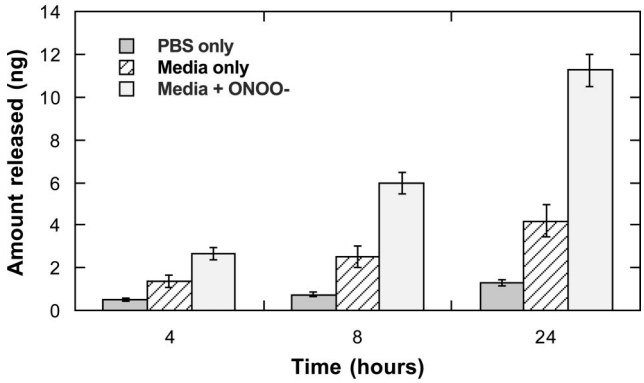

Figure 5. Release of covalently attached Alexa Fluor 488 from porous Si microparticles as a function of time in various solutions, demonstrating ROS-triggered release. The release rate is smallest in PBS buffer, intermediate in cell media, and greatest in cell media containing 1 mM SIN-1, which generates the strong oxidant peroxynitrite *in situ*. The data are quantified by fluorescence spectrometry of the supernatant solution, using a calibration curve for the emission of Alexa Fluor 488 at 516 nm in either PBS or in cell media with an excitation of 495 nm.

in the efficiency of excited state energy transfer between the attached dye and the porous Si matrix. The present interpretation is consistent with the previous work in the porous Si and porous SiO_2 systems.[38−40,47,48]

The dye molecules tethered to the porous Si matrix release into the solution as a result of the Si surface oxidation. It is well-established that the silicon−carbon bonds produced by hydrosilylation of porous Si are quite stable in aqueous media.[21,30] Oxidation of the porous Si matrix produces Si−O back bonds (eq 5) that are more susceptible to hydrolysis. In this work, the hydrolysis-induced release of the attached fluorophore was studied in PBS, cell media, and cell media containing added $ONOO^-$. Appearance of fluorophore in solution was quantified by fluorescence spectrometry.

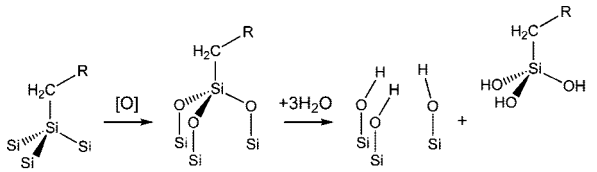

(3)

R = Alexa Fluor 488 or doxorubicin

Addition of an oxidant can be used to trigger the release of molecules covalently attached to porous Si microparticles (Figure 5). In a 4 h period, the amount of fluorophore released from porous Si microparticles immersed in cell media is 2 times the amount released from microparticles immersed in aqueous PBS buffer. When $ONOO^-$ is added to microparticles immersed in cell media, the amount of Alexa Fluor 488 released is 4 times the amount released when in PBS. The increased amount of fluorophore released in cell media compared to PBS is attributed to a greater rate of oxidation due to the presence of amines and surfactants in the cell media.[49−52] The presence of $ONOO^-$ in the cell media further accelerates the rate of oxidation. After 24 h, there is >2-fold increase in the concentration of fluorophore in a solution medium containing $ONOO^-$ compared to media alone and >10-fold increase compared to PBS.

The oxidation-triggered hydrolysis reaction that releases the dye into solution is potentially useful for drug delivery applications. Previous work using porous Si as a drug delivery material has focused on using physical adsorption as a means to load drug, often resulting in rapid, burst-type release profiles.[9,10] Covalent attachment offers a means to prolong the period of release and to harness physiological stimuli to modify the rate of release.

In order to test the relevance of the present approach to realistic therapeutic conditions, the anticancer drug doxorubicin was loaded into porous Si microparticles by covalent attachment, and release into PBS solutions held at 37 °C was quantified. Two particle preparations were used. The first preparation was rinsed with methanol after covalent attachment of the drug, and the second was rinsed with water. It was found that doxorubicin is not sufficiently soluble in water to allow efficient removal of the free drug with a water rinse. Thus particles with covalently attached doxorubicin that were rinsed with water contained both covalently bound and physically adsorbed doxorubicin. The temporal drug release profiles of the two covalent preparations were quantified and compared with profiles from samples in which doxorubicin was loaded solely by physical adsorption (Figure 6). Approximately 75 μg of doxorubicin was loaded per milligram of particles in the covalent attachment protocols, with 45 μg/mg remaining after the methanol rinse; the physical adsorption protocol resulted in a doxorubicin loading of approximately 55 μg/mg.

For particles loaded with doxorubicin through physical adsorption, a burst of drug release is observed within the first 2 h, and all detectable drug is released within 24 h. Particles containing a combination of covalently attached and physisorbed doxorubicin (the water-rinsed samples) display a smaller initial burst followed by a gradual release over a period of ~24 h. Particles loaded with doxorubicin through covalent attachment and rinsed with methanol to remove all physisorbed drug display a continuous, slower release of doxorubicin that lasts for >5 days. For all three sample types, the measured quantity of doxorubicin released into solution is less than the amount that is initially loaded into the microparticles. The discrepancy is attributed to chemical degradation of doxorubicin during the course of the experiments, as doxorubicin is known to be moderately unstable in aqueous media at pH 7.[53]

Cellular assays were performed to determine if the released doxorubicin retains its functional toxicity.

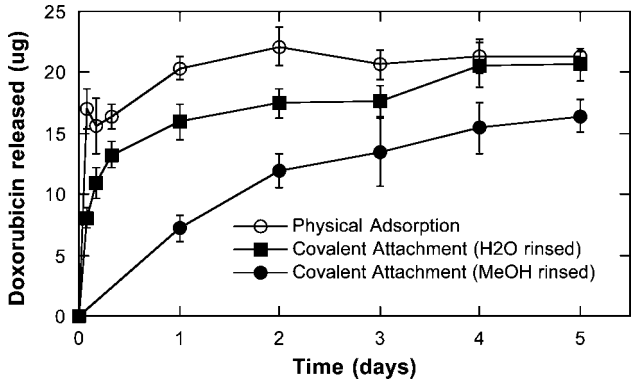

Figure 6. Release of doxorubicin from porous Si microparticles into PBS buffer. Complete drug release occurs within 1 day for doxorubicin loaded through physical adsorption, while the covalently attached drug is continuously released for >5 days. The data are quantified by fluorescence spectrometry of the supernatant solution, monitoring the excitation spectrum between 500 and 650 nm and calculating the concentration based on a calibration curve for the emission at 580 nm using an excitation of 470 nm.

Doxorubicin is somewhat unstable in aqueous solutions at pH 7, and in addition, the chemical modification used to attach the molecule to the porous Si host microparticles may interfere with doxorubicin's mode of action. An MTT (3-(4,5-dimethylthiazol-2-yl)-2,5-diphenyl tetrasodium bromide) toxicity assay was used to test cell viability. Cells were exposed to free doxorubicin (dox), empty porous Si microparticles (PSiMPs), and porous Si microparticles in which doxorubicin was loaded by covalent attachment (dox-pSiMPs). The samples of doxorubicin and porous Si microparticles were added to HeLa cells and assessed for cytotoxicity 48 h after exposure (Figure 7). The viability of cells exposed to doxorubicin-loaded porous Si microparticles was significantly lower than cells exposed to empty porous Si microparticles and somewhat higher than cells exposed to the same quantity of free doxorubicin. Porous Si microparticle samples in which doxorubicin is loaded by physisorption display toxicity similar to the covalently attached material. It should be noted that porous Si is able to reduce MTT in the absence of cells, giving rise to an apparent lack of toxicity with this particular mitochondrial activity assay.[54,55] Thus the significant toxicity observed for doxorubicin-loaded porous Si microparticles is likely to be an underestimate of the actual cellular toxicity. Similar results are observed using the SRB (sulforhodamine B) assay (Supporting Information Figure 1), which quantifies protein production as a measure of cellular viability. Both assays indicate that doxorubicin released from porous Si microparticles retains significant functional toxicity.

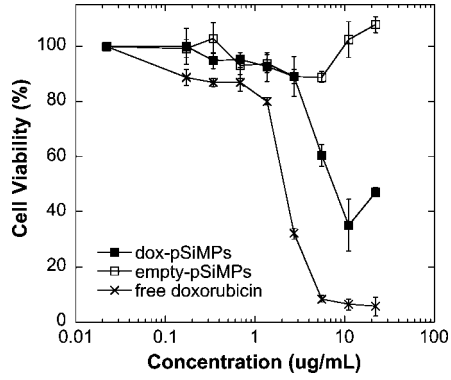

Figure 7. Viability of HeLa cells (MTT assay) after exposure to free doxorubicin, empty porous Si microparticles (empty-pSiMPs), and porous Si microparticles loaded with doxorubicin by covalent attachment (dox-pSiMPs). The *x*-axis displays the doxorubicin concentration in terms of the total amount of doxorubicin added per milliliter of media. For the empty microparticles, there is no doxorubicin loaded, but a mass of particles equal to the mass of doxorubicin-loaded microparticles is used (1 μg/mL on the *x*-axis corresponds to 46 μg of particles). The mass loading of the doxorubicin-loaded microparticles is 22 ng of doxorubicin per microgram of particles. Toxicity assessed 48 h after sample introduction.

As mentioned above, doxorubicin is unstable in aqueous media, and it is possible that the drug may react chemically with porous Si microparticles either before or after release. In addition, the chemical attachment method employed modifies the drug from its normal form. Indeed, HPLC-MS analysis of the supernatant from doxorubicin-loaded porous Si microparticles indicates the presence of degradation products as well as compounds that can be ascribed to doxorubicin with the chemical tether attached (Supporting Information Figure S1). Compared with physical adsorption, the covalent attachment method allows prolonged release of drug in a controllable fashion, although the attachment chemistry requires modification of the molecular structure of the drug. Thus the type of drugs that can be used with this approach may be somewhat limited.

In conclusion, loading of small molecules into mesoporous Si microparticles can be accomplished by covalent attachment *via* Si−C bonding. The molecules are released into aqueous solutions in a two-step mechanism involving oxidation and subsequent dissolution of the porous Si matrix. When a fluorescent dye is used, energy transfer quenching provides a sensitive probe of the oxidation process; fluorescence intensity of attached dye increases as the porous nanostructure oxidizes from semiconducting Si to insulating SiO_2, and the intensity of fluorescence from the solution increases as the porous matrix dissolves and dye is released. The covalent attachment method was tested with the anticancer drug doxorubicin, and release of the active drug was verified by the MTT cellular viability assay. Exposure of molecule-loaded porous Si particles to a reactive oxygen species (ROS) such as peroxynitrite results in triggered release of the attached molecule. This method allows the grafted molecule to be released only when the covalent bonds are broken or when the matrix is degraded. Because elevated levels of ROS are often generated in the vicinity of diseased or tumor tissues, the triggered release mechanism presented in this paper is relevant to medical therapeutic applications.

EXPERIMENTAL METHODS

Synthesis of Porous Si Microparticles. Porous Si microparticles were prepared from the electrochemical etching of highly doped, (100)-oriented, p-type Si wafers (boron-doped, ~1 mΩ resistivity) in a 3:1 solution of 48% aqueous hydrofluoric acid (HF)/ethanol (HF from Fisher, Inc. CAUTION: HF is highly toxic and contact with skin should be avoided). A Si wafer with an exposed area of 3.2 cm^2 was contacted on the back side with a strip of aluminum foil and mounted in a Teflon etching cell with a platinum counter electrode. The wafer was etched at a constant current density of 248 mA/cm^2 for 2 min. The resulting porous layer was then lifted off by electropolishing in 3.33% HF in ethanol solution for 2 min at a current density of 6.2 mA/cm^2. The etching and electropolishing procedure was repeated four times per wafer, and the resulting porous layers were ultrasonicated in ethanol for 20 min.

Hydrosilylation of Porous Si Microparticles. Approximately 25 mg of the porous Si microparticles prepared in the manner described above was placed in a 10 mL Pyrex beaker and immersed in 1 mL of undecylenic acid (95%, purchased from Sigma-Aldrich). The microparticles in undecylenic acid were then heated in a commercial consumer microwave oven (Sears Kenmore 700 W) for 4 min at 280 W. The particles were then rinsed with hexane and ethanol to remove excess undecylenic acid.

Loading of Alexa Fluor 488 and Doxorubicin into Porous Si Microparticles. For loading of Alexa Fluor 488 (Invitrogen), approximately 4 mg of porous Si microparticles was suspended in 500 μL of ethanol. Afterward, 5 μL of a 2 mg/mL solution of Alexa Fluor 488 in water and 25 μL of a 10 mg/mL solution of *N*-(3-dimethylaminopropyl)-*N*2-ethylcarbodiimide hydrochloride or EDAC (commercial grade, Sigma-Aldrich Chemicals) were added. The microparticles were then agitated for 2 h at room temperature and rinsed thoroughly with PBS. Doxorubicin hydrochloride (Sigma-Aldrich Chemicals) was loaded into porous Si microparticles in a similar manner. Approximately 4 mg of porous Si microparticles was suspended in 500 μL of 10% dimethyl sulfoxide (DMSO) in Dulbecco's phosphate buffered saline (PBS) solution. Afterward, 200 μL of a 1 mg/mL solution of doxorubicin in water and 150 μL of a 10 mg/mL solution of EDAC were added. The particles were then agitated for 2 h at room temperature and rinsed with methanol five times.

Physical Characterization of Porous Si Microparticles. SEM images were obtained using a Phillips XL30 ESEM field emission gun (FEG) electron microscope operating at an accelerating voltage of 20 kV. Diffuse reflectance mode Fourier transform infrared (FTIR) spectra were obtained with a Nicolet-Magna 550 spectrometer. Nitrogen adsorption−desorption isotherms of porous Si microparticles were recorded at 77 K using a Micromeritics ASAP 2010 volumetric apparatus. Prior to the adsorption experiment, approximately 30 mg of porous Si samples was outgassed overnight *in situ* at 313 K. The surface area of the sample was measured by the BET (Brunnauer−Emmett−Teller) method, which yields the amount of adsorbate corresponding to a molecular monolayer. The pore dimensions were determined using the BdB (Broekhof−de Boer) method from the nitrogen adsorption curve.[32−34]

Microscopy. Fluorescent images were obtained using the Nikon Eclipse LV150 microscope with a Photometrics HQ^2 camera. For all acquired images, a 10× objective with a numerical aperture of 30 was used. Fluorescence images were acquired with either 50 or 100 ms exposure times. Measurement of fluorescence intensity of Alexa Fluor 488 was achieved using an excitation filter wavelength of 540−580 nm and an emisison filter wavelength of 600−660 nm. The computer program MetaMorph from Molecular Devices Operation was used for image acquisition, processing, and analysis.

Determination of Drug Loading. Porous Si microparticles were completely dissolved in a solution of 1 M KOH for 10 min. The solution was then neutralized with an equal volume of 1 M HCl to recover the fluorescence spectrum of free dye or drug. A Perkin-Elmer LS50B fluorescence spectrometer was used for fluorescence measurements. For measurement of the amount of dye loaded, the solution was excited at 495 nm and the emission from 500 to 600 nm was measured. The peak was found to be at 520 nm, and the concentration was calculated based on a calibration curve. For doxorubicin, the solution was excited at 470 nm and the intensity of the emission spectrum was measured between 500 and 650 nm. A calibration curve for the emission at 580 nm was used to calculate the amount of doxorubicin loaded (Supporting Information Figure 3).

***In Vitro* Release Studies.** Porous Si microparticles were rinsed thoroughly with PBS prior to drug release studies. 3-Morpholinosydnomine (SIN-1) purchased from Invitrogen, which generates superoxide and NO, was used to produce a flux of peroxynitrite. Approximately 600 μg of porous Si microparticles loaded with Alexa Fluor 488 was placed in a 35 mm Petri dish and suspended with either PBS, cell media (DMEM), or cell media with 1 mM concentration of SIN-1. They were incubated at 37 °C and agitated at 50 rpm, and 1 mL of the release medium was removed at various time intervals to determine the amount of dye released. Fresh PBS, cell media, or cell media containing SIN-1 (depending on the relevant experiment) was added back to the release solution to maintain a constant volume. Concentrations of the samples were determined by measuring the fluorescence intensity of the released dye with an excitation of 495 nm. The peak intensity of Alexa Fluor 488 was found to be at 516 nm, and a calibration curve for the dye in PBS or in cell media was used to determine the amount of dye released in their respective medium (Supporting Information Figure 3). For doxorubicin release studies, approximately 2 mg of porous Si microparticles was placed in 15 mL of PBS solution at 37 °C and agitated at 100 rpm. At predetermined time intervals, 2 mL of the release medium was removed and was replaced with fresh medium. Drug concentration in the release samples was determined as in the drug loading determinations.

Cell Toxicity Assay. The HeLa cell line was utilized for cell toxicity experiments. Cells were routinely maintained at 37 °C in 5% CO_2 in DMEM culture medium. In preparation for the MTT assay, the cells were plated in a 96-well plate. Fifty microliters of porous Si particle dispersions or free doxorubicin solution of the requisite concentrations was introduced to each well with 100 μL of media. To perform the MTT assay, the media was removed after a 48 h incubation period and the wells were rinsed with 100 μL of PBS three times. MTT solution was added to each well and allowed to react for 4 h at 37 °C. MTT formazan crystals were then dissolved in the MTT solvent. Values were determined by subtracting the absorbance value measured at 690 nm from the value measured at 570 nm. A larger MTT-absorbance-minus-background value indicates a larger relative viability.

Acknowledgment. This material is based upon work supported by the National Cancer Institute of the National Institutes of Health (NIH) under Grant U54 CA 119335, and by the National Science Foundation under Grant No. DMR-0806859. The CNRS/DREI program (call for proposal CNRS/United States 2005 #3312) is acknowledged for financial support of scientist exchanges. M.J.S. is a member of the Moores UCSD Cancer Center and the UCSD NanoTUMOR Center. The authors thank Joseph Kinsella for help with sample preparation and discussions, Ryan Anderson of the UCSD Integrated Technology Laboratory for assistance in scanning electron microscopy, Corine Tourne-Peteilh and Francesco Di Renzo of Intitut Charles Gerhardt Montepllier for helpful discussions and for assistance with generating nitrogen adsorption isotherms, and Yongxuan Su for assistance with HPLC-MS analysis.

Supporting Information Available: SRB cell viability assay results, HPLC-MS traces of supernatants from microparticles soaked in PBS solution, calibration curves for fluorescence assays. This material is available free of charge *via* the Internet at http://pubs.acs.org.

REFERENCES AND NOTES

1. Tao, S. L.; Desai, T. A. Microfabricated Drug Delivery Systems: From Particles to Pores. *Adv. Drug Delivery Rev.* **2003**, *55*, 315–328.

2. Grayson, A. C. R.; Choi, I. S.; Tyler, B. M.; Wang, P. P.; Brem, H.; Cima, M. J.; Langer, R. Multi-Pulse Drug Delivery from a Resorbable Polymeric Microchip Device. *Nat. Mater.* **2003**, *2*, 767–772.
3. Brayden, D. J. Controlled Release Technologies for Drug Delivery. *Drug Discovery Today* **2003**, *8*, 976–978.
4. Torchilin, V. P. Recent Advances with Liposomes as Pharmaceutical Carriers. *Nat. Rev. Drug Discovery* **2005**, *4*, 145–160.
5. Torchilin, V. P. Micellar Nanocarriers: Pharmaceutical Perspectives. *Pharm. Res.* **2007**, *24*, 1–16.
6. Van Vlerken, L. E.; Duan, Z. F.; Seiden, M. V.; Amiji, M. M. Modulation of Intracellular Ceramide Using Polymeric Nanoparticles to Overcome Multidrug Resistance in Cancer. *Cancer Res.* **2007**, *67*, 4843–4850.
7. Devalapally, H.; Chakilam, A.; Amiji, M. M. Role of Nanotechnology in Pharmaceutical Product Development. *J. Pharm. Sci.* **2007**, *96*, 2547–2565.
8. Bégu, S.; Durand, R.; Lerner, D. A.; Charnay, C.; Tourné-Peteilh, C.; Devoisselle, J.-M. Preparation and Characterization of Silicious Material Using Liposomes as Template. *Chem. Commun.* **2003**, 640–641.
9. Salonen, J.; Kaukonen, A. M.; Hirvonen, J.; Lehto, V.-P. Mesoporous Silicon in Drug Delivery Applications. *J. Pharm. Sci.* **2008**, *97*, 632–653.
10. Anglin, E. J.; Cheng, L.; Freeman, W. R.; Sailor, M. J. Porous Silicon in Drug Delivery Devices and Materials. *Adv. Drug Delivery Rev.* **2008**, *60*, 1266–1277.
11. Canham, L. T. Bioactive Silicon Structure Fabrication Through Nanoetching Techniques. *Adv. Mater.* **1995**, *7*, 1033–1037.
12. Canham, L. T.; Reeves, C. L.; Loni, A.; Houlton, M. R.; Newey, J. P.; Simons, A. J.; Cox, T. I. Calcium Phosphate Nucleation on Porous Silicon: Factors Influencing Kinetics in Acellular Simulated Body Fluids. *Thin Solid Films* **1997**, *297*, 304–307.
13. Coffer, J. L.; Montchamp, J. L.; Aimone, J. B.; Weis, R. P. Routes to Calcified Porous Silicon: Implications for Drug Delivery and Biosensing. *Phys. Status Solidi A* **2003**, *197*, 336–339.
14. Foraker, A. B.; Walczak, R. J.; Cohen, M. H.; Boiarski, T. A.; Grove, C. F.; Swaan, P. W. Microfabricated Porous Silicon Particles Enhance Paracellular Delivery of Insulin Across Intestinal Caco-2 Cell Monolayers. *Pharm. Res.* **2003**, *20*, 110–116.
15. Vaccari, L.; Canton, D.; Zaffaroni, N.; Villa, R.; Tormen, M.; di Fabrizio, E. Porous Silicon as Drug Carrier for Controlled Delivery of Doxorubicin Anticancer Agent. *Microelectron. Eng.* **2006**, *83*, 1598–1601.
16. Rosengren, A.; Wallman, L.; Bengtsson, M.; Laurell, T. H.; Danielsen, N.; Bjursten, L. M. Tissue Reactions to Porous Silicon: A Comparative Biomaterial Study. *Phys. Status Solidi A* **2000**, *182*, 527–531.
17. Bayliss, S. C.; Buckberry, L. D.; Harris, P. J.; Tobin, M. Nature of the Silicon-Animal Cell Interface. *J. Porous Mater.* **2000**, *7*, 191–195.
18. Coffer, J. L.; Whitehead, M. A.; Nagesha, D. K.; Mukherjee, P.; Akkaraju, G.; Totolici, M.; Saffie, R. S.; Canham, L. T. Porous Silicon-Based Scaffolds for Tissue Engineering and Other Biomedical Applications. *Phys. Status Solidi A* **2005**, *202*, 1451–1455.
19. Cheng, L.; Anglin, E.; Cunin, F.; Kim, D.; Sailor, M. J.; Falkenstein, I.; Tammewar, A.; Freeman, W. R. Intravitreal Properties of Porous Silicon Photonic Crystals: A Potential Self-Reporting Intraocular Drug Delivery Vehicle. *Br. J. Ophthalmol.* **2008**, *92*, 705–711.
20. Zhang, X. G. Morphology and Formation Mechanisms of Porous Silicon. *J. Electrochem. Soc.* **2004**, *151*, C69–C80.
21. Buriak, J. M. Organometallic Chemistry on Silicon and Germanium Surfaces. *Chem. Rev.* **2002**, *102*, 1272–1308.
22. Anderson, S. H. C.; Elliott, H.; Wallis, D. J.; Canham, L. T.; Powell, J. J. Dissolution of Different Forms of Partially Porous Silicon Wafers under Simulated Physiological Conditions. *Phys. Status Solidi A* **2003**, *197*, 331–335.
23. Evered, D.; O'Connor, M. *Silicon Biochemistry*; Wiley: Chichester, UK, 1986; p 264.
24. Salonen, J.; Laitinen, L.; Kaukonen, A. M.; Tuura, J.; Bjorkqvist, M.; Heikkila, T.; Vaha-Heikkila, K.; Hirvonen, J.; Lehto, V. P. Mesoporous Silicon Microparticles for Oral Drug Delivery: Loading and Release of Five Model Drugs. *J. Controlled Release* **2005**, *108*, 362–374.
25. Anglin, E. J.; Schwartz, M. P.; Ng, V. P.; Perelman, L. A.; Sailor, M. J. Engineering the Chemistry and Nanostructure of Porous Silicon Fabry-Pérot Films for Loading and Release of a Steroid. *Langmuir* **2004**, *20*, 11264–11269.
26. Harris, T. J.; von Maltzahn, G.; Derfus, A. M.; Ruoslahti, E.; Bhatia, S. N. Proteolytic Actuation of Nanoparticle Self-Assembly. *Angew. Chem., Int. Ed.* **2006**, *45*, 3161–3165.
27. Minotti, G.; Menna, P.; Salvatorelli, E.; Cairo, G.; Gianni, L. Anthracyclines: Molecular Advances and Pharmacologic Developments in Antitumor Activity and Cardiotoxicity. *Pharmacol. Rev.* **2004**, *56*, 185–229.
28. Cunin, F.; Schmedake, T. A.; Link, J. R.; Li, Y. Y.; Koh, J.; Bhatia, S. N.; Sailor, M. J. Biomolecular Screening with Encoded Porous Silicon Photonic Crystals. *Nat. Mater.* **2002**, *1*, 39–41.
29. Gupta, P.; Dillon, A. C.; Bracker, A. S.; George, S. M. FTIR Studies of H_2O and D_2O Decomposition on Porous Silicon. *Surf. Sci.* **1991**, *245*, 360–372.
30. Lees, I. N.; Lin, H.; Canaria, C. A.; Gurtner, C.; Sailor, M. J.; Miskelly, G. M. Chemical Stability of Porous Silicon Surfaces Electrochemically Modified with Functional Alkyl Species. *Langmuir* **2003**, *19*, 9812–9817.
31. Boukherroub, R.; Petit, A.; Loupy, A.; Chazalviel, J. N.; Ozanam, F. Microwave-Assisted Chemical Functionalization of Hydrogen-Terminated Porous Silicon Surfaces. *J. Phys. Chem. B* **2003**, *107*, 13459–13462.
32. Gregg, S. J.; Sing, K. S. W. *Adsorption, Surface Area and Porosity*, 2nd ed.; Academic Press Inc.: London, 1982; p 112.
33. Brunauer, S.; Emmett, P. H.; Teller, E. Adsorption of Gases in Multimolecular Layers. *J. Am. Chem. Soc.* **1938**, *60*, 309–319.
34. Broekhof, J. C.; Deboer, J. H. Studies on Pore Systems in Catalysts 0.9. Calculation of Pore Distributions from Adsorption Branch of Nitrogen Sorption Isotherms in Case of Open Cylindrical Pores. a. Fundamental Equations. *J. Catal.* **1967**, *9*, 8.
35. Socrates, G. *Infrared and Raman Characteristic Group Frequencies: Tables and Charts*, 3rd ed.; John Wiley & Sons Ltd.: New York, 2001.
36. Snee, P. T.; Somers, R. C.; Nair, G.; Zimmer, J. P.; Bawendi, M. G.; Nocera, D. G. A Ratiometric CdSe/ZnS Nanocrystal pH Sensor. *J. Am. Chem. Soc.* **2006**, *128*, 13320–13321.
37. Somers, R. C.; Bawendi, M. G.; Nocera, D. G. CdSe Nanocrystal Based Chem-/Bio-Sensors. *Chem. Soc. Rev.* **2007**, *36*, 579–591.
38. Setzu, S.; Solsona, P.; Létant, S.; Romestain, R.; Vial, J. C. Microcavity Effect on Dye Impregnated Porous Silicon Samples. *Eur. Phys. J.* **1999**, *7*, 59–63.
39. Setzu, S.; Létant, S.; Solsona, P.; Romestain, R.; Vial, J. C. Improvement of the Luminescence in P-Type As-Prepared or Dye Impregnated Porous Silicon Microcavities. *J. Lumin.* **1998**, *80*, 129–132.
40. Letant, S.; Vial, J. C. Energy Transfer in Dye Impregnated Porous Silicon. *J. Appl. Phys.* **1997**, *82*, 397–401.
41. Bruska, A.; Chernook, A.; Hietschold, M.; von Borczyskowski, C. Spectroscopic and SEM Investigations of Porous Silicon Doped with Dyes. *Appl. Surf. Sci.* **1996**, *102*, 427–430.
42. Canham, L. T. Laser Dye Impregnation of Oxidized Porous Si on Si Wafers. *Appl. Phys. Lett.* **1993**, *63*, 337–339.
43. Squadrito, G. L.; Pryor, W. A. The Formation of Peroxynitrite *In Vivo* from Nitric Oxide and Superoxide. *Chem. Biol. Interact.* **1995**, *96*, 203–206.
44. Nagaraj, S.; Gupta, K.; Pisarev, V.; Kinarsky, L.; Sherman, S.; Kang, L.; Herber, D. L.; Schneck, J.; Gabrilovich, D. I. Altered Recognition of Antigen is a Mechanism of CD8+ T Cell Tolerance in Cancer. *Nat. Med.* **2007**, *13*, 828–835.

45. Bonfoco, E.; Krainc, D.; Ankarcrona, M.; Nicotera, P.; Lipton, S. A. Apoptosis and Necrosis: Two Distinct Events Induced, Respectively, By Mild and Intense Insults with *N*-methyl-D-aspartate or Nitric Oxide/Superoxide in Cortical Cell Cultures. *Proc. Natl. Acad. Sci. U.S.A.* **1995**, *92*, 7162–7166.
46. Martin-Romero, F. J.; Gutierrez-Martin, Y.; Henao, F.; Gutierrez-Merino, C. Fluorescence Measurements of Steady State Peroxynitrite Production Upon SIN-1 Decomposition: NADH *versus* Dihydrodichlorofluorescein and Dihydrorhodamine 123. *J. Fluoresc.* **2004**, *14*, 17–23.
47. Chouket, A.; Elhouichet, H.; Boukherroub, R.; Oueslati, M. Porous Silica-Laser Dye Composite: Physical and Optical Properties. *Phys. Status Solidi A* **2007**, *204*, 1518–1522.
48. Gole, J. L.; DeVincentis, J. A.; Seals, L. Optical Pumping of Dye-Complexed and -Sensitized Porous Silicon Increasing Photoluminescence Emission Rates. *J. Phys. Chem. B* **1999**, *103*, 979–987.
49. Canaria, C. A.; Huang, M.; Cho, Y.; Heinrich, J. L.; Lee, L. I.; Shane, M. J.; Smith, R. C.; Sailor, M. J.; Miskelly, G. M. The Effect of Surfactants on the Reactivity and Photophysics of Luminescent Nanocrystalline Porous Silicon. *Adv. Funct. Mater.* **2002**, *12*, 495–500.
50. Sweryda-Krawiek, B.; Chandler-Henderson, R. R.; Coffer, J. L.; Rho, Y. G.; Pinizzotto, R. F. A Comparison of Porous Silicon and Silicon Nanocrystallite Photoluminescence Quenching with Amines. *J. Phys. Chem.* **1996**, *100*, 13776–13780.
51. Chandler-Henderson, R. R.; Sweryda-Krawiec, B.; Coffer, J. L. Steric Considerations In The Amine-Induced Quenching Of Luminescent Porous Silicon. *J. Phys. Chem.* **1995**, *99*, 8851–8855.
52. Thomas, J. C.; Pacholski, C.; Sailor, M. J. Delivery of Nanogram Payloads Using Magnetic Porous Silicon Microcarriers. *Lab Chip* **2006**, *6*, 782–787.
53. Chavanpatil, M. D.; Khdair, A.; Patil, Y.; Handa, H.; Mao, G.; Panyam, J. Polymer-Surfactant Nanoparticles for Sustained Release of Water-Soluble Drugs. *J. Pharm. Sci.* **2007**, *96*, 3379–3389.
54. Low, S. P.; Williams, K. A.; Canham, L. T.; Voelcker, N. H. Evaluation of Mammalian Cell Adhesion on Surface-Modified Porous Silicon. *Biomaterials* **2006**, *27*, 4538–4546.
55. Laaksonen, T.; Santos, H.; Vihola, H.; Salonen, J.; Riikonen, J.; Heikkila, T.; Peltonen, L.; Kumar, N.; Murzin, D. Y.; Lehto, V.-P.; Hirvonen, J. Failure of MTT as a Toxicity Testing Agent for Mesoporous Silicon Microparticles. *Chem. Res. Toxicol.* **2007**, *20*, 1913–1918.